A FIRST DETERMINATION OF THE POSITION OF THE 'DOPPLER' PEAK

Stephen Hancock and Graca Rocha
MRAO, Cambridge,UK.

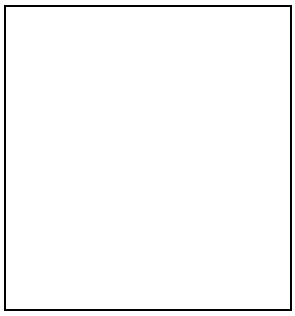

Abstract

Cosmological theories for the origin and evolution of structure in the Universe are highly predictive of the form of the angular power spectrum of cosmic microwave background fluctuations. We present new results from a comprehensive study of CMB observations which provide the first measurements of the power spectrum all the way down to angular scales of ~ 10 arcminutes. On large scales a joint likelihood analysis of the COBE and Tenerife data fixes the power spectrum normalisation to be $Q_{rms-ps} = 21.0 \pm 1.6\mu$K for an initially scale invariant spectrum of fluctuations. The combined data are consistent with this hypothesis, placing a limit of $n = 1.3 \pm 0.3$ on the spectral slope. On intermediate scales we find clear evidence for a 'Doppler' peak in the power spectrum localised in both angular scale and amplitude. This first estimate of the angular position of the peak is used to place a new direct limit on the curvature of the Universe, corresponding to a density of $\Omega = 0.7^{+1.0}_{-0.4}$. Very low density open Universe models are inconsistent with this limit unless there is a significant contribution from a cosmological constant.

1 Introduction

Observations of the Cosmic Microwave Background (CMB) radiation provide information about epochs and physical scales that are inaccessible to conventional astronomy. In contrast to traditional methods of determining cosmological parameters, which rely on the combination of results from local observations[31], CMB observations provide direct measurements[5, 48] over cosmological scales, thereby avoiding the systematic uncertainties and biases associated with conventional techniques. Assuming that the fluctuations conform to a random Gaussian field, then all of the statistical properties are contained in the angular power spectrum and consequently tracing out the form of the CMB power spectrum is a key goal of observational

cosmology[5, 3, 4, 40, 22, 24, 33]. CMB observations on different angular scales are probing different physical effects (see White *et al.* 1995 [48] and Scott *et al.* 1995 [40] for comprehensive reviews). On scales $\gtrsim 2^\circ$, which is the size of the horizon at last scattering of the CMB photons, the gravitational redshifting of the CMB photons through the Sachs-Wolfe effect is the dominant process. The presence of either a background of primordial gravity waves and/or mass fluctuations at recombination, would lead to fluctuations in the CMB. The scalar mass density fluctuations lie outside the horizon and are predicted by inflationary theory to have a scale-invariant flat power spectrum *i.e.* $n = 1$. In Section 2 we use the combined large scale COBE and Tenerife observations to delimit the spectral slope n and to fix the power spectrum normalisation Q_{rms-ps}.

On scales of $\sim 0.2^\circ - 2.0^\circ$ the scattering of the CMB photons during acoustic oscillations of the photon-baryon fluid at recombination [13] is expected to imprint characteristic 'large' amplitude peaks into the CMB power spectrum. The position l_p of the main peak reflects the size of the horizon at last scattering of the CMB photons and is determined almost entirely by the geometry of the Universe. As a result one finds that [22, 23] l_p depends directly on the density of the Universe according to $l_p \propto 1/\sqrt{\Omega}$. The height of the peak is directly proportional to the fractional mass in baryons Ω_b and also varies according to the expansion rate of the Universe as specified by the Hubble constant H_0; in general [22] for baryon fractions $\Omega_b \lesssim 0.05$, increasing H_0 reduces the peak height whilst the converse is true at higher baryon densities. Consequently by measuring the amplitude of the intermediate scale CMB fluctuations relative to the CMB fluctuations resulting from scalar density perturbations on large scales we can trace out the CMB power spectrum and hence directly estimate Ω, Ω_b and H_0 from the position and amplitude of the main peak. In Section 3, we use current CMB observations, including new data from the CAT, Tenerife and COBE experiments to build up a conservative and consistent picture of the CMB power spectrum on large and intermediate scales and hence to obtain a first estimate of both the position and amplitude of the Doppler peak.

2 Joint likelihood analysis of COBE and Tenerife observations

Both the COBE satellite observations [2] and the ground-based observations from the Tenerife experiments [11] are on sufficiently large angular scales that they probe fluctuations that are beyond the horizon scale at recombination and are hence still in the linear growth regime. Such data can therefore be used to investigate the spectral slope of the initial primordial fluctuation spectrum generated in the early Universe. Numerous attempts [42, 19, 20, 45, 2, 16] have been made to determine both the slope and normalisation of the power spectrum at small multipoles. The approach detailed in Hancock *et al.* [19] and reviewed here differs from previous analyses in that for the first time the COBE and Tenerife data have been used *together* taking into account *all* correlations between the two data sets. This method, developed in collaboration with Max Tegmark, uses a direct brute force calculation of the likelihood function for the combined data.

We apply the likelihood analysis to the COBE two-year [1] data and the Tenerife dec $+40^\circ$ scan [19, 20], assuming a power law model with free parameters n and Q_{rms-ps}. The COBE Galaxy-cut two-year map consists of 4038 pixels, whilst the Tenerife Galaxy cut (RA $161^\circ - 230^\circ$) scan contains 70 pixels, requiring a 4108×4108 covariance matrix for a joint likelihood analysis of the data. We arrange the pixels in a 4108-dimensional vector $\mathbf{\Delta T} = (\Delta T_1, \Delta T_2, ...\Delta T_{4108})$ and compute the likelihood function $L(n, Q_{rms-ps}) \propto \exp -(\mathbf{\Delta T^T V^{-1} \Delta T})$ as in Tegmark and Bunn 1995 [45] by Cholesky decomposition of the 4108×4108 covariance matrix $\mathbf{V}$ at a dense grid of points in the (n, Q_{rms-ps})-parameter space, marginalizing over the four "nuisance parameters" that describe the monopole and dipole. The covariance matrix consists of three

parts: a 70×70 block with the covariance between the Tenerife pixels, a 4038×4038 block with the covariance between the COBE pixels, and off-diagonal 4038×70 blocks containing the covariance between the Tenerife and COBE pixels. In this way, we fully account for intrinsic correlations due to the CMB structure and correlations due to sampling with the different instruments. Additionally in forming the likelihood function we have intrinsically incorporated the effects of cosmic and sample variance for the two data sets, plus random noise and the interdependence of the model parameters.

The resulting normalised joint likelihood function depicted in Figure 4 of Hancock *et al.* (submitted [19]) thus provides an accurate description of the constraints placed on n and Q_{rms-ps} by the joint data set. The likelihood is seen to peak at $n = 1.37$, $Q_{rms-ps} = 16.1\mu$K, with a 68% confidence region (uniform prior) encompassing 0.90 to 1.73 in n for Q_{rms-ps} in the range from 12.1 to 22.9 μK. Margenalising over Q_{rms-ps} one finds $n = 1.3 \pm 0.3$, whilst conditioning on $n = 1$, one finds a power spectrum normalisation of $Q_{rms-ps} = 21.0 \pm 1.6$. These results using COBE 2-year and Tenerife dec $+40^\circ$ data are comparable to those obtained using the COBE 4-year data [2], for which $n = 1.2 \pm 0.3$ and $Q_{rms-ps} = 18 \pm 1.6\mu$K for $n = 1$. The joint analysis of the COBE 4-year data plus a significantly extended Tenerife sky area is in progress and is expected to improve on these limits. However, it is clear that the current Tenerife and COBE results offer a consistent picture on large scales and do not favour values of n less than unity. In the case of power law inflation, such large values of n do not allow for a significant contribution from tensor modes, giving us confidence in normalising the scalar power spectrum to the large scale anisotropy data. In the following, we will *assume* that this is the case and will proceed to compare the large and intermediate scale anisotropy measurements to test for the presence of a Doppler peak.

3 The CMB Power Spectrum

Reconstructing the CMB power spectrum over large and intermediate angular scales requires the simultaneous use of data from a number of different experiments, all with their own classes of uncertainties. At the time of writing, there are numerous CMB experiments operating worldwide, and it is appropriate here to restrict ourselves to the subset of experiments which have produced conclusive evidence for the detection of CMB anisotropy. Clear detections have now been reported by a number of different groups, using observations from satellites (COBE[42, 2]), ground-based switching experiments (Tenerife[19],[20], Python[36], South Pole[17], Saskatoon[30]), balloon mounted instruments (ARGO[12], MAX[44], MSAM[6, 7]) and more recently ground-based interferometer telescopes (CAT[41]). Given the difficulties inherent in observing CMB anisotropy, it is possible and indeed likely, that some of these results are contaminated by foreground effects[35]. Determining the form of the CMB power spectrum in order to trace out the Doppler peak requires a careful, in-depth consideration of the CMB measurements from the different experiments within a common framework as presented in Hancock *et al.* (submitted [21]); the full details including a discussion of foreground contamination are presented in Rocha *et al.* (in preparation[35]). In this paper and the following contribution [34], we present our principal findings. We consider all of the latest CMB measurements, including new results from COBE, Tenerife, MAX, Saskatoon and CAT, with the exception of the MSAM results and the MAX detection in the Mu Pegasi region which is contaminated by dust emission[14]. On the largest scales corresponding to small l, new COBE [2] and Tenerife [19] results improve the power spectrum normalisation, whilst significant gains in knowledge at high l are provided by new results from the Saskatoon and CAT experiments. The full data set spans a range of 2 to ~ 700 in l, sufficient to test for the main Doppler peak out to $\Omega = 0.1$.

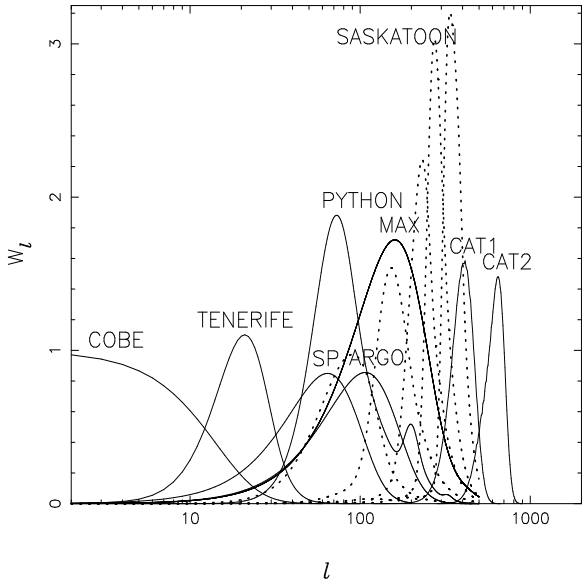

Figure 1: The experimental window functions W_l.

3.1 The flat bandpower approximation

The competing models for the origin and evolution of structure predict[5, 22], the shape and amplitude of the CMB power spectrum and its Fourier equivalent, the autocorrelation function $C(\theta) =< \Delta T(\mathbf{n_1})\Delta T(\mathbf{n_2}) >$ where $\mathbf{n_1} \cdot \mathbf{n_2} = \cos\theta$. Expanding the intrinsic angular correlation function $C(\theta)$ in terms of spherical harmonics one obtains: $C(\theta) = \sum_{l\geq 2}^{\infty}(2l+1)C_l P_l(\cos(\theta))/4\pi$, where low order multipoles l correspond to large angular scales θ and large l-modes are equivalent to small angles on the sky. The different experiments sample different l-modes according to their window functions W_l, as shown in Figure 1 : for a detailed discussion of window functions see [47, 46]. The observed power in CMB fluctuations as seen through a window W_l is given by

$$C_{obs}(0) = \left(\frac{\Delta T_{obs}}{T}\right)^2 = \sum_{l\geq 2}^{\infty}(2l+1)C_l W_l/4\pi. \quad (1)$$

The C_l are predicted by the cosmological theories and contain all of the relevant statistical information for models described by Gaussian random fields[5]. Given W_l, then for the C_l's corresponding to the theoretical model under consideration it is possible to obtain the value of ΔT_{obs} one would expect to observe using the chosen experiment. This value can then be compared to the value actually observed to test the cosmological model.

We take the reported CMB detections and convert them to a common framework of flat bandpower results[3, 4] as given in Table 1 of the contribution by Rocha and Hancock (this volume). In order to use the observed anisotropy levels to place constraints on the CMB power spectrum one must in general know the form of the C_l under test. However, in most cases the form of C_l can be represented by a flat spectrum $C_l \propto C_2/(l(l+1))$ over the width of a given experimental window, so that the bandpower is $\Delta T_l/T = \sqrt{C_{obs}(0)/I(W_l)}$, where we define $I(W_l)$ according to Bond (1995)[3, 4] as $I(W_l) = \sum_{l=2}^{\infty}(l+0.5)W_l/(l(l+1)$. This bandpower estimate is centred on the effective multipole $l_e = I(lW_l)/I(W_l)$. In many instances experimenters now report results directly for a flat spectrum and when this is not so we have converted the quoted power in fluctuations into the equivalent flat band estimate. Each group has obtained limits on the intrinsic anisotropy level using a likelihood analysis (see *e.g.* Hancock *et al.* 1994[20]), which incorporates uncertainties due to random errors, sampling variance[39] and cosmic variance[38, 37]. The form of the likelihood function is not necessarily Gaussian, and

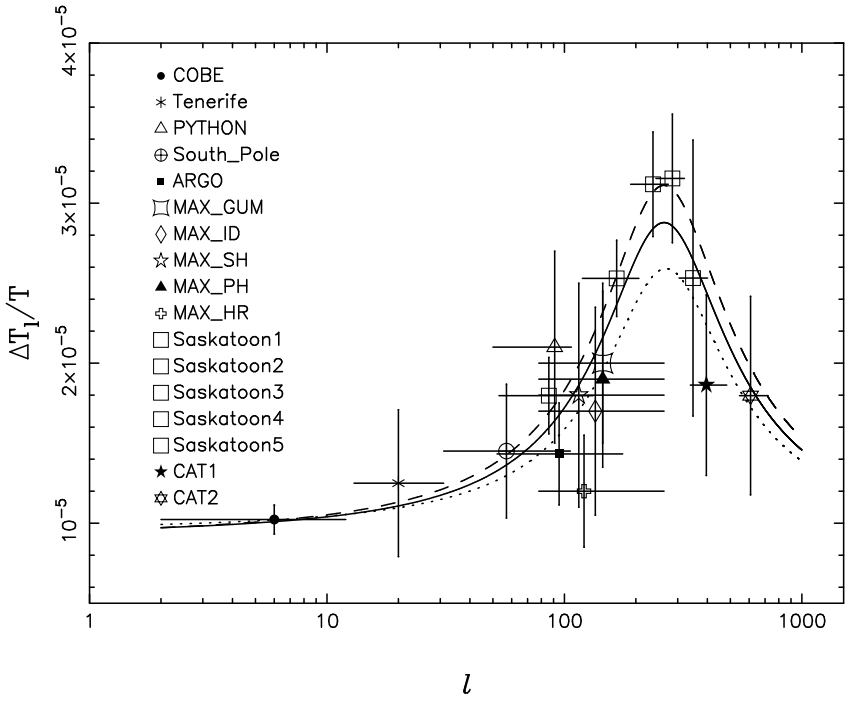

Figure 2: The data points from Table 1 (see [34]) are shown compared to the best fit analytical CDM model. The dotted and dashed lines show the best fit models which are obtained when the Saskatoon calibration is adjusted by ±14%. The data points from the MAX experiment are shown offset in l for clarity

strictly one requires a method that will utilise the full likelihood functions from all experiments consistently. However, given the relatively large error bars on most of the reported data points it is sufficient for our purposes here to approximate all likelihood results as originating from a Gaussian distribution, giving the one-sigma error bounds in column three of Table 1 (see [34]) by averaging the difference in the reported 68% upper and lower limits and the best fit ΔT_l. This bias introduced by this averaging is discussed in [35].

Results from the MSAM experiment are not included here, because they do not provide an independent measure of the power spectrum since their angular sensitivity and sky coverage are already incorporated within the Saskatoon measurements. Netterfield *et al.* [30] report good agreement between the MSAM double difference results and Saskatoon measurements, although the discrepancy with the MSAM single difference data is yet to be resolved.

3.2 Estimating the parameters of the Doppler Peak

The data points from Table 1 (see [34]) are plotted in Figure 2, in which the horizontal bars represent the range of l contributing to each data point. There is a noticeable rise in the observed power spectrum at $l \simeq 200$, followed by a fall at higher l, tracing out a clearly defined peak in the spectrum. In the past several groups [40, 24, 33] have attempted to determine the presence of a Doppler peak, but only now are the data sufficient to make a first detection and to put constraints on the closure parameter Ω. As a first step, we adopt a simple three parameter model of the power spectrum, which we find adequately accounts for the properties of the principal Doppler peak for both standard Cold Dark Matter (CDM) models [10, 13] and open Universe ($\Omega < 1$) models [24]. The functional form chosen is a modified version of that

used in Scott, Silk & White [40] — we choose the following:

$$l(l+1)C_l = 6C_2 \left(1 + \frac{A_{peak}}{1+y(l)^2}\right) / \left(1 + \frac{A_{peak}}{1+y(2)^2}\right) \quad (2)$$

where $y(l) = (\log_{10} l - log_{10}(220/\sqrt{\Omega}))/0.266$. In this representation C_2 specifies the power spectrum normalisation, whilst the first Doppler peak has height A_{peak} above C_2, width $\log_{10} l = 0.266$ and for $\Omega = 1.0$ is centred at $l \simeq 220$. By appropriately specifying the parameters C_2, A_{peak} and Ω it is possible to reproduce to a good approximation the C_l spectra corresponding to standard models of structure formation with different values of Ω, Ω_b and H_0. Such a form will not reproduce the structure of the *secondary* Doppler peaks, but we have checked the model against the overall form of the $\Omega = 1$ models of Efstathiou and the open models reported in Kamionkowsky *et al.* [24] and find that this form adequately reflects the properties of the main peak. This satisfies our present considerations since the current CMB data are not yet up to the task of discriminating the secondary peaks. Varying the three model parameters in equation (2) we form C_l spectra corresponding to a range of cosmological models, which are then used in equation (1) to obtain a simulated observation for the ith experiment, before converting to the bandpower equivalent result $\Delta T_l[C_2, A_{peak}, \Omega](i)$. The chi-squared for this set of parameters is given by

$$\chi^2(C_2, A_{peak}, \Omega) = \sum_{i=1}^{nd} \frac{(\Delta T_l^{obs}(i) - \Delta T_l[C_2, A_{peak}, \Omega](i))^2}{\sigma_i^2},$$

for the nd data points in Table 1 (see [34]) and the relative likelihood function is formed according to $L(C_2, A_{peak}, \Omega) \propto \exp(-\chi^2(C_2, A_{peak}, \Omega)/2)$. We vary the power spectrum normalisation C_2 within the 95 % limits for the COBE 4-year data [2] and consider A_{peak} in the range 0 to 30 and values of the density parameter up to $\Omega = 5$. The data included in the fit are those from Table 1 (see [34]), which with the exception of Saskatoon include uncertainties in the overall calibration. There is a $\pm 14\%$ calibration error in the Saskatoon data, but since the Saskatoon points are not independent this will apply equally to all five points [30]. The likelihood function is evaluated for three cases: (i) that the calibration is correct, (ii) the calibration is the lowest allowed value and (iii) the calibration is the maximum allowed value. In each case the likelihood function is marginalised over C_2 before calculating limits on the remaining two parameters according to Bayesian integration with a uniform prior.

4 Results and Discussion

In Fig. 3 the likelihood function obtained from fitting the model C_l spectra to the data of Table 1 (see [21]) is shown plotted as a function of the amplitude and position (Ω) of the Doppler peak. The highly peaked nature of the likelihood function in Fig. 3 is good evidence for the presence of a Doppler peak localised in both position (Ω) and amplitude. In Fig. 4 we show the 1-D conditional likelihood curve for Ω, obtained by cutting through the surface shown in Fig. 3 at the best-fit value of A_{peak}. The best fit value of Ω is 0.7 with an allowed 68% range of $0.30 \leq \Omega \leq 1.73$.

In Figure 2 the best fit model, represented by the solid line, is shown compared to the data points, assuming no error in the calibration of the Saskatoon observations. The chi-squared per degree of freedom for this model is 0.9, implying a good fit to the data. The peak lies at $l = 263^{+139}_{-94}$ corresponding to a density parameter $\Omega = 0.70^{+1.0}_{-0.4}$; the height of the peak is $A_{peak} = 9.0^{+4.5}_{-2.5}$. The dashed and dotted lines show the best fit models ($\Omega = 0.70^{+0.92}_{-0.37}$,

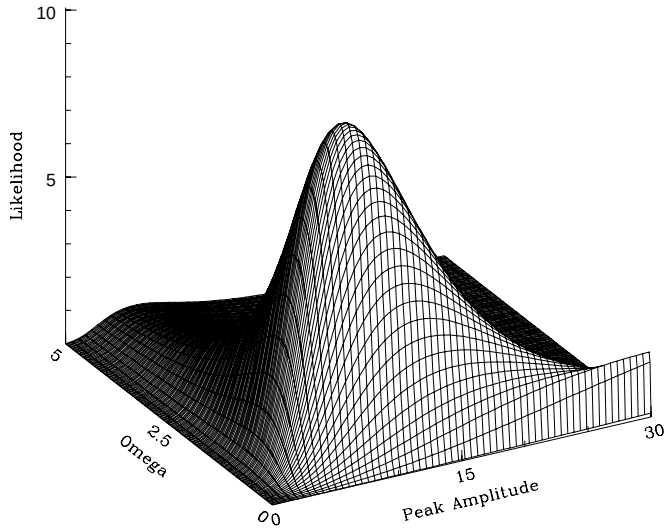

Figure 3: The likelihood surface for Ω and A_{peak}. (The nominal Saskatoon calibration is assumed.)

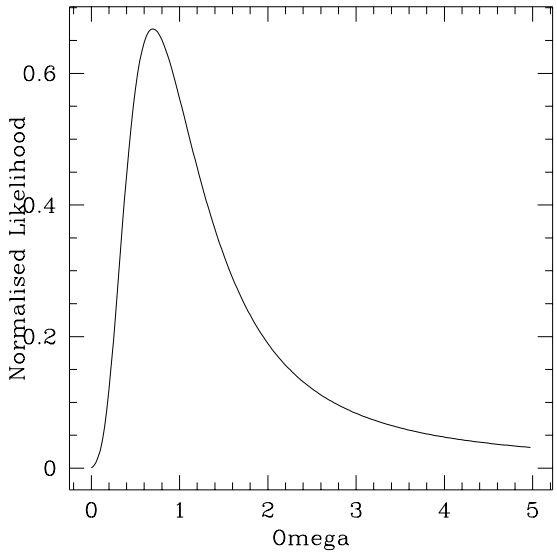

Figure 4: The 1-D conditional likelihood curve for Ω.

$A_{peak} = 11.0^{+5.0}_{-4.0}$ and $\Omega = 0.68^{+1.2}_{-0.4}$, $A_{peak} = 6.5^{+3.5}_{-2.0}$ respectively) assuming that the Saskatoon observations lie at the upper and lower end of the permitted range in calibration error. These likelihood results using the analytic form for the C_l and the results from a more detailed analysis using exact models (see Hancock *et al.* submitted [21]; Rocha and Hancock, this volume) imply that independent of calibration uncertainties in the data, current CMB data are inconsistent with cosmological models with $\Omega < 0.3$.

5 Conclusions

Our current results provide good evidence for the Doppler peak, verifying a crucial prediction of cosmological models and providing an interesting new measurement of fundamental cosmological parameters. In Rocha *et al.* [35], a detailed comparison of the CMB data is made with the theoretical power spectra predicted by a range of flat, tilted, reionized, open models and models with non-zero cosmological constant. The existence of the Doppler peak has important consequences for the future of CMB astronomy, implying that our basic theory is correct and that improving our constraints on cosmological parameters is simply a matter of improved instrumental sensitivity and ability to separate out foregrounds. New instruments such as VSA [26], MAP and the proposed COBRAS/SAMBA satellite [29] will provide this improved sensitivity and should delimit Ω and other parameters with unprecedented precision.

Acknowledgements. Thanks to all the members of the CAT and Tenerife teams for their help and assistance in this work. and to B. Netterfield for supplying the Saskatoon window functions. S. Hancock wishes to acknowledge a Research Fellowship at St. John's College, Cambridge, U.K.

References

[1] Bennett, C.L. et al. 1994, ApJ., 436, 423

[2] Bennett C.L. *et al.* , 1996, ApJ., 464, L1

[3] Bond J.R., 1995, "*Cosmology and Large Scale Structure*" ed. Schaeffer, R. Elsevier Science Publishers, Netherlands, Proc. Les Houches School, Session LX, August 1993

[4] Bond, J.R., Astrophys. Lett. and Comm., in press

[5] Bond, J.R., Efstathiou, G.P., 1987, MNRAS, 226, 655

[6] Cheng E.S. *et al.* , 1994, ApJ., 422, L37

[7] Cheng E.S. *et al.* , 1996, ApJ., 456, L71

[8] Copi C.J., Schramm D.N., Turner M.S., 1995, Science, 267, 192

[9] Crittenden, R., Bond, J.R., Davis, R.L., Efstathiou, G., Steinhardt, P.J., 1993, Phys. Rev. Lett., 71, 324

[10] Davis, M., Efstathiou, G., Frenk, C.S., White, S.D.M, 1992, Nature, 356, 489

[11] Davies, R.D. et al. 1996, MNRAS, 278, 883

[12] De Bernardis P. *et al.* , 1994, ApJ., 422, L33

[13] Efstathiou, G.P., 1987, in "*Physics of the Early Universe*", proceedings of the thirty-sixth Scottish Universities Summer School in physics 1989, ed. by Peacock *et al.*

[14] Fischer, M.L. *et al.* , 1995, ApJ., 444, 226

[15] Freedman, W.L. *et al.* , 1994, Nature, 371, 757

[16] Gorski, K.M. et al. 1994, ApJ., 430, L89

[17] Gundersen, J.O *et al.* ,1995, ApJ., 443 L57

[18] Guth, A.H., 1981, Phys. Rev. D, 23, 347

[19] Hancock, S. *et al.* , submitted to MNRAS

[20] Hancock, S. *et al.* , 1994, Nature, 367, 333

[21] Hancock, S., Rocha, G., Lasenby, A.N. and Gutierrez, C.M., submitted to MNRAS

[22] Hu W., Sugiyama N., 1995, ApJ., 444, 489

[23] Kamionkowsky, M. *et al.* , 1994a, ApJ., 426, L57

[24] Kamionkowsky, M. *et al.* , 1994b, ApJ., 434, L1

[25] Kennicutt, R.C., Freedman, W.L., Mould, J.R., 1995, ApJ., 110, 1476

[26] Lasenby, A.N., Hancock, S., 1995, Proc. of : *"Current Topics in Astrofundamental Physics: The Early Universe"*, p327, eds. Sanchez, N., Zichichi, A., Kluwer

[27] Liddle, A.R., Lyth, D.H., 1992, Phys. Letters, B291, 391

[28] Magueijo, J. Albrecht, A., Coulson, D., Ferreira, P., Phys. Rev. Lett., in press

[29] Mandolesi, N. *et al.* , 1995, Planetary and Space Science, 43, 1459

[30] Netterfield C.B. *et al.* , submitted to ApJ.

[31] Ostriker, J.P., Steinhardt, P.J., 1995, Nature, 377, 600

[32] Pierce, M.J. *et al.* , 1994, Nature, 371, 385

[33] Ratra, B. *et al.* , submitted to ApJ. Lett.

[34] Rocha, G. and Hancock, S. this volume.

[35] Rocha, G., Hancock, S., Lasenby, A.N., Gutierrez, C.M. in preparation.

[36] Ruhl, J.E. *et al.* , 1995, ApJ., 453, L1

[37] Scaramela N., Vittorio N., 1990, ApJ., 353, 372

[38] Scaramela N., Vittorio N., 1993, ApJ., 411, 1

[39] Scott D., Srednicki M., White M., 1994, ApJ., 241, L5

[40] Scott D., Silk, J., White, M., 1995, Science, 268, 5212

[41] Scott, P.F. *et al.* , 1996, ApJ., 461, L1

[42] Smoot, G.F. *et al.* , 1992, ApJ., 396, L1

[43] Steinhardt, P., 1993, *Proc. of the Yamada Conference XXXVII "Evolution of the Universe and its Observational Quest"*, p159

[44] Tanaka, S.T. *et al.* , submitted to ApJ.

[45] Tegmark, M., & Bunn, E.F. 1995, ApJ., 455, 1

[46] White M., Srednicki M., 1995, ApJ., 443, 6

[47] White M., Krauss L.M., Silk J., 1993, ApJ., 418, 535

[48] White, M., Scott, D., Silk, J., 1994, Ann. Rev. Astron. Astrophys., 32, 319